Applied Surface Science 426 (2017) 1182–1189

Contents lists available at ScienceDirect

Applied Surface Science

journal homepage: www.elsevier.com/locate/apsusc

Full Length Article

Theoretical study of new potential semiconductor surfaces performance for dye sensitized solar cell usage: TiO_2-B (001), (100) and $H_2Ti_3O_7$ (100)

Estefania German[a,b,**], Ricardo Faccio[b,*], Álvaro W. Mombrú[b]

[a] Departamento de Física, Universidad Nacional del Sur & IFISUR (UNS-CONICET), Av. Alem 1253, 8000, Bahía Blanca, Argentina
[b] Centro NanoMat-DETEMA, Facultad de Química, Universidad de la República, Uruguay

ARTICLE INFO

Article history:
Received 14 July 2017
Received in revised form 29 July 2017
Accepted 1 August 2017
Available online 2 August 2017

Keywords:
Dye sensitized solar cells
DFT
TiO2 polymorphs
Hidrogen titanates
Solar cells

ABSTRACT

Hydrogen titanate ($H_2Ti_3O_7$) and TiO_2-B polymorph are potential surfaces identified experimentally in the last years, which need to be analyzed. To study their performance as surfaces for dye sensitized solar cells (DSSC), a set of dye adsorption configurations were evaluated on them, as model dye the small and organic catechol molecule was used. We have calculated adsorption geometry, energy, electronic transfer from dye to semiconductor adsorbent and frontier orbitals by means of density functional theory (DFT). Results show that vacancy-like defected $H_2Ti_3O_7$ (100) and TiO_2-B (100) surfaces present favorable adsorption energies. Finally, an adequate energy level alignment make both surfaces prone to be adequate for direct electron transfer upon excitation, from catechol to the conduction band of the semiconductors, with bands located in the Visible region of the electromagnetic spectrum. Additionally, the band structure alignment indicates an increase in the open circuit voltage, in reference to I_2/I_3^- redox pair potential. All these characteristics make hydrogen titanate ($H_2Ti_3O_7$) and TiO_2-B polymorph promising for DSSC applications.

1. Introduction

The TiO_2-B polymorph was synthesized by Marchand et al. [1], its chemical structure presents bronze pattern Na_xTiO_2, presenting continuous channels and lower density than the others TiO_2 polymorphs, i.e. anatase, rutile, brookite. It can be obtained easily via soft chemical routes by proton exchange followed by dehydratation of titanates in layers, as Feist et al. have reported [2,3]. Different nanostructural morphologies of TiO_2-B have been synthesized as nanoparticles [4], nanowires [5–7], nanoribbons [8] and nanotubes [9]. However, regarding its performance in DSSC, as far as we know, only few studies have been reported [4,8,10] with comparable results.

Only some theoretical studies have been carried out regarding TiO_2-B polymorph. Structural, electronic and vibrational properties have been calculated by first principles DFT [11]. Vittadini et al. have studied the reconstruction and structural stability of TiO_2-B surfaces [12]. Adsorption of water on TiO_2-B (001) and (100) has been reported by Liu et al. [13]. The presence of TiO_2-B during synthesis of titania nanostructures, showing a stability similar to that for anatase at nanoscale level, together with few results reported about this polymorph, motivate us to study these surfaces.

Nanostructured TiO_2 can be found in several forms, like sheets, rods and scrolls and it can interconvert into each other changing the chemical setting, temperature and/or pressure [14–16]. These transformations can create nanostructures with different size, shape, structure, and also variable compositions [17]. These compositions can vary from stoichiometric TiO_2 to metal-ion and proton-exchanged titanates [14]. One interesting reversible interconversion is between $Na_2Ti_3O_7$ nanowire and $H_2Ti_3O_7$ nanoscrolls resulting from changes of pH in aqueous dispersions [18,19]. TiO_2 in phase anatase and protonated titanates $H_2Ti_3O_7$-type are directly related structurally and rearrangement from one specie to other is possible changing local water partial pressure [15]. In literature, we can find few experimental researches regarding $H_2Ti_3O_7$ structure and properties [20,21], as well as theoretical reports [22,23]. To the best of our knowledge, this compound is gaining interest and it has not been studied yet as a surface.

* Corresponding author
** Corresponding author at: Centro NanoMat-DETEMA, Facultad de Química, Universidad de la República, Uruguay.
E-mail addresses: egerman@uns.edu.ar (E. German), rfaccio@fq.edu.uy, rjfaccio@gmail.com (R. Faccio).

http://dx.doi.org/10.1016/j.apsusc.2017.08.012
0169-4332/

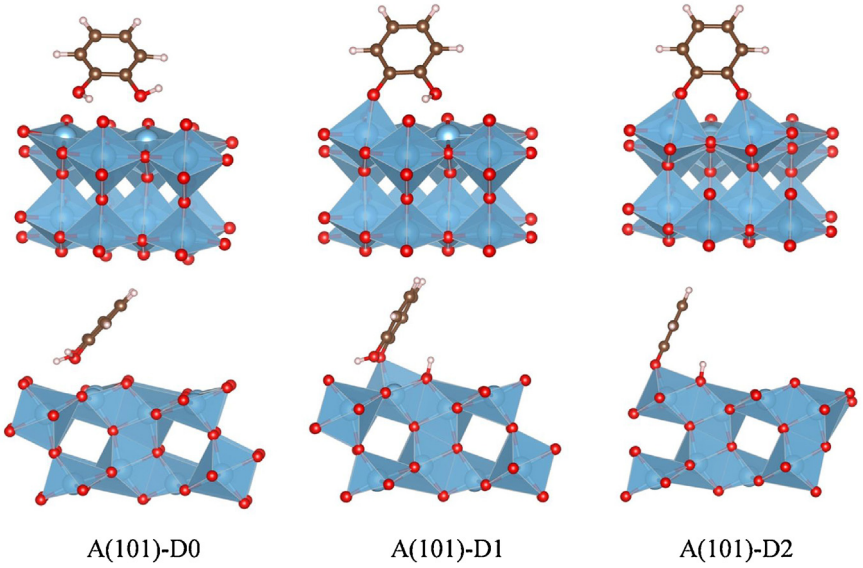

Fig. 1. Catechol adsorption on anatase (101), molecular adsorption D0, mono-dentate adsorption D1 and bi-dentate adsorption D2. Front and side views.

The aim of this work is to study the performance of these new TiO_2-B and $H_2Ti_3O_7$ surfaces in dye sensitized solar cells (DSSC) [24], given that TiO_2 polymorphs are nontoxic, cheap and photostable semiconductors. These DSSCs are promising material for harvesting solar energy, very attractive due to its low cost, high efficiency, simple fabrication process and for being environmentally friendly [25–28].

As testing dye, we have used catechol, which is the smallest molecular sensitizer and presents two hydroxyl groups for attaching to the semiconductor surface, these features make it an excellent model to study the surfaces performance in DSSC [29–34]. As it was made previously for several authors for anatase and rutile polymorphs [35–46].

2. Computational methods

In all calculations, Density Functional Theory (DFT) [47] implemented in the Vienna Ab-initio Simulation Package (VASP) was used [48]. The projector augmented wave (PAW) method [49,50] was employed to account for the electron–ion core interaction, using the Perdew-Burke-Ernzerhof (PBE) as the generalized gradient approximation (GGA) [51] for the exchange-correlation term. In order to treat the strong on-site Coulomb interaction of localized electrons in transition metal oxides, which is not properly described by the GGA (and LDA) approach and affects the electronic structure, the GGA + U method proposed by Dudarev et al. [52] was used. Setting a U-parameter of 4 eV for 3d level of Ti in TiO_2-B polymorph and a U-parameter of 5 eV in hydrogen titanate [53], the multiple occupation of d-orbitals is penalized, and thus, the band gap width takes values closer than the experimental ones, attenuating the underestimation of this width, as well as the electron delocalization.

The space groups for TiO_2-B and $H_2Ti_3O_7$ are C2/m [11,21] and surfaces were modeled by cutting the unit cells in the specific directions to obtain the different faces, and then a vacuum region along the non-periodical direction was applied, of about 10 Å which is large enough to avoid significant interactions between different images of the slab. We have selected the following surfaces for catechol adsorption: $H_2Ti_3O_7$ (100), TiO_2-B (001) and (100). During adsorption, a fully slab relaxation was allowed for the first two system, for TiO_2-B (100) the superficial two layers were allowed to move and the bottom three were kept frozen in the bare surface positions. The Brillouin-zone was sampled using $4 \times 4 \times 1$ Monkhorst-Pack K-point mesh [54]. A cutoff energy of 400 eV was used for the plane-wave basis set. Model-dye adsorption energy was calculated using the following equation:

$$E_{ads} = -(E_{catechol/surface} - E_{catechol} - E_{surface})$$

being $E_{catechol/surface}$ the energy of the system dye/semiconductor, $E_{catechol}$ stands for the energy of isolated dye molecule calculated in a cubic box of $10 \times 10 \times 10$ Å^3 and $E_{surface}$ represents the energy of the bare – non-interacting – semiconductor surface. A positive E_{ads} implies a favorable energy process, while a negative implies the opposite, in order to compare our results with those reported in literature.

Density of states curves (DOS) were calculated to evaluate the electron transfer from the dye valence band to the semiconductor conduction band in the different systems under study, and they were plotted to check the band gap width estimation. HOMO and LUMO frontier orbitals were drawn for the more promising adsorption systems. In order to understand and evaluate appropriately how these new surfaces perform as adsorbents for DSSCs, our results are compared with those for the well-known catechol/anatase (101) system [37,41,46].

Finally, for the most stable geometries we performed further vibrational analysis by getting phonons at Γ – *point*. In all the cases, we obtained real frequencies demonstrating that all the geometries correspond to local minima, see supporting information for Table of vibrational frequencies.

3. Results and discussion

3.1. Dye-semiconductor systems

3.1.1. Catechol on anatase (101)

Although this system is widely studied, we have carried out this calculation as a fine tuning of the mechanics employed. We have taken into account three different possible adsorption sites, namely D0, D1 and D2 which correspond to molecular adsorption, mono-dentate adsorption with dissociation of one H atom and bi-dentate adsorption with dissociation of both H atoms from catechol hydroxyl groups, respectively, as it can be seen in Fig. 1.

It was found that the more probable adsorption site for catechol, energetically is D2, followed by D1 and at last D0, with adsorption

Table 1
Ti_{surf}—O_{dye} and O_{surf}—H_{dye} bond lengths in Å, catechol adsorption energy and energy gap from valence band to conduction band in eV for the three sites studied in catechol/anatase (101) system.

	Ti—O (Å)	O—H (Å)	E ads (eV)	VB-CB (eV)
D0	2.51 2.35		0.431	2.911
D1	1.94 2.33	0.972	0.810	2.101
D2	1.91 1.91	0.972 0.974	0.903	1.604

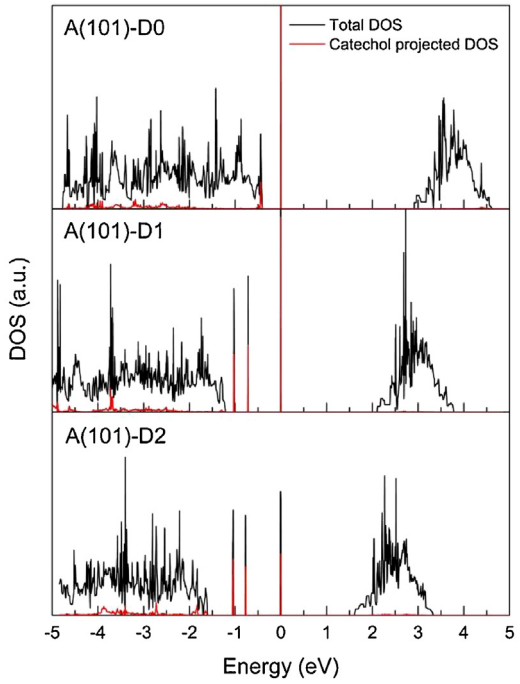

Fig. 2. Projected density of states for total system and catechol, for D0, D1 and D2 adsorption configuration on anatase (101).

energies of 0.903, 0.810 and 0.431 eV, respectively. This tendency agrees with data reported in literature [37,41,46], as seen in Table 1. The smaller electronic gap from valence band to conduction band also corresponds to D2 adsorption configuration, having a value of 1.604 eV. These two aspects, energetic and electronic, make the D2 configuration the more appropriate for dye adsorption, which is the same conclusion reached in previous cited literature.

In Fig. 2, the DOS curves are shown, the catechol projected DOS is colored in red. In the three cases, valence band energy states correspond to model-dye and they are located at the Fermi level. Also, it can be seen in Fig. 2 that while the molecule is being adsorbed, the VB-CB gap is shortened, from 2.911 eV to 1.604 eV, being best located in the visible region of the electromagnetic spectrum.

3.1.2. Catechol on $H_2Ti_3O_7$ (100)

The same adsorption configurations are studied for hydrogen titanate surface, i.e. D0, D1, D2 and a new one called C, which consists in the bonding of two oxygen atoms from catechol with one titanium surface atom (chelating bond) and dissociation of both H atoms from hydroxyl groups of the adsorbate. These systems are energetically unfavorable with the exception of the one corresponding to molecular adsorption, D0. However, when DOS curves are calculated and plotted we found that the energy gap from VB to CB is high, around 2.536 eV, making this system not feasible for DSSC usage.

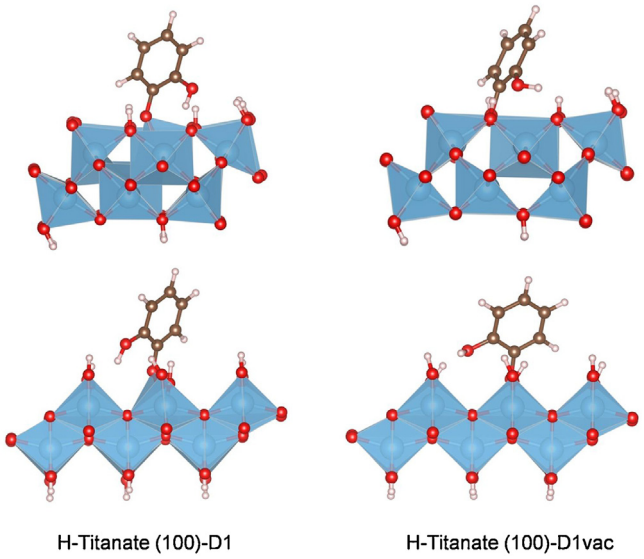

Fig. 3. Catechol adsorption on $H_2Ti_3O_7$ (100), D1 mono-dentate adsorption and D1-vac mono-dentate adsorption with dye oxygen atom located in surface O-vacancy. Front and side views.

Table 2
Ti_{surf}—O_{dye} and O_{surf}—H_{dye} bond lengths in Å, catechol adsorption energy and energy gap from valence band to conduction band in eV for the two sites studied in catechol/$H_2Ti_3O_7$ (100) system.

	Ti-O (Å)	O—H (Å)	E ads (eV)	VB-CB (eV)
D1	1.95	0.974	1.096	1.624
D1-vac	2.06 2.11	0.972	1.750	2.354

In order to turn the surface more reactive, an oxygen vacancy is generated [20] and two catechol adsorption modes are studied. D1, which corresponds to the mono-dentate adsorption, a H atom from the dye is dissociated and the other one is kept bonded to the adsorbate. D1-vac corresponds to the adsorption of catechol forcing its oxygen atom to set in the superficial O-vacancy, bonding equally to two Ti atoms from the semiconductor surface. These configurations are shown in Fig. 3, and data regarding their bond lengths, adsorption energies and VB-CB energy gaps are summarized in Table 2.

Giving that these two configurations are optimum for catechol adsorption, it is interesting to calculate their respective DOS curves. In Fig. 4 the DOS curves are shown (the catechol projected DOS is in red). Despite energetically D1-vac configuration is more probable to happen, D1 configuration has the shorter energetic gap from VB to CB, better suitable for DSSC applications [55,56].

3.1.3. Catechol on TiO_2-B (001)

We have considered four dye adsorption configurations for TiO_2-B polymorph (001) surface, namely, D0, D2, C1 and C2. The last two configurations are described by the bonding of two dye-oxygen atoms to one superficial titanium atom, the difference between C1 and C2 is where the dissociated H atoms are located on the surface, as it is shown in Fig. 5. In Table 3 structural information as well as energetic data are listed for each configuration. None of these are energetically probable to occur.

In Fig. 6 we can see that the gap from VB to CB for configuration D2 is 0.919 eV, and for C1 is 1.384 eV, which is better than the 1.604 eV found for anatase (101) and better than 1.624 eV found for hydrogen titanate, very convenient for DSSC applications since it involves both the visible and the infrared region of the electromag-

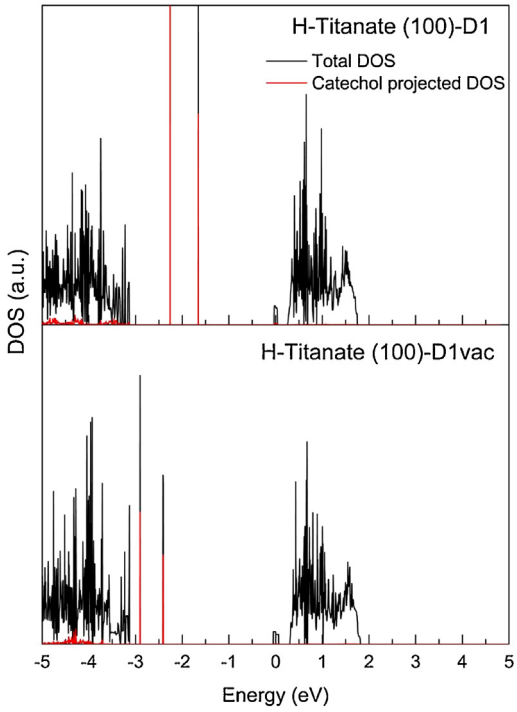

Fig. 4. Total and projected DOS curves for catechol adsorption on $H_2Ti_3O_7$ surface containing an oxygen vacancy.

netic spectrum [55,56]. However, its dye adsorption energy makes this system not appropriate for our aim. The reason for this behavior is the low surface energy of facet (001) of TiO_2-B polymorph, which clearly reduces its chemical reactivity, which compromises the adsorption of the dye.

3.1.4. Catechol on TiO_2-B (100)

For the case of catechol adsorbed on TiO_2-B polymorph (100) surface, we have studied the same four configurations that in the previous case (D0, D2, C1 and C2), as seen in Fig. 7.

Table 3
Ti_{surf}—O_{dye} and O_{surf}—H_{dye} bond lengths in Å, catechol adsorption energy and energy gap from valence band to conduction band in eV for the four sites studied in catechol/TiO_2-B (001) system.

	Ti—O (Å)	O—H (Å)	E ads (eV)	VB-CB (eV)
D0	2.73 2.89		−0.111	1.197
D2	1.92 1.92	0.976 0.976	−0.489	0.919
C1	2.01 2.08	0.978 0.989	−1.488	1.384
C2	2.02 2.02	0.980 0.979	−1.693	1.571

Table 4
Ti_{surf}—O_{dye} and O_{surf}—H_{dye} bond lengths in Å, catechol adsorption energy and energy gap from valence band to conduction band in eV for the four sites studied in catechol/TiO_2-B (100) system.

	Ti-O (Å)	O—H (Å)	E ads (eV)	VB-CB (eV)
D0	2.464 2.226		0.395	2.931
D2	1.879 1.879	0.980 0.980	1.068	2.938
C1	1.942 1.972	0.978 0.979	0.285	0.637
C2	1.961 1.956	0.978 0.972	0.804	2.918

In Table 4, structural and energetic information is listed for the four adsorption configurations. All cases are probable to occur energetically, following the sequence D2, C2, D0 and C1 with adsorption energies of 1.068, 0.804, 0.395 and 0.285 eV, respectively. Nevertheless, only the C1 case has a convenient energy gap between VB and CB for DSSC applications, but it worths to notice that its adsorption energy is minor than that on anatase (101) and hydrogen titanate containing an O vacancy. The VB-CB gaps have been plotted in Fig. 8, total DOS and catechol projected DOS are shown.

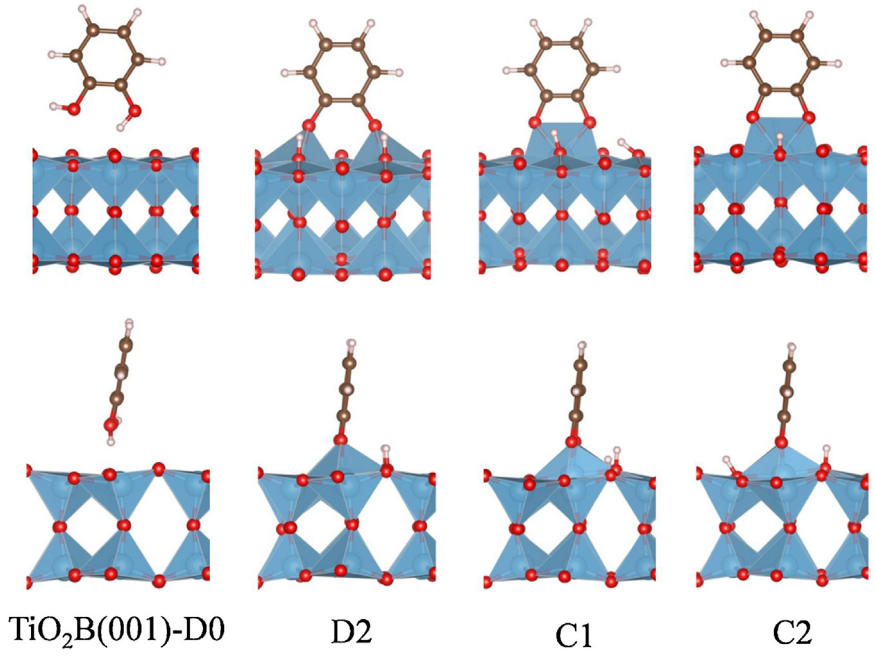

Fig. 5. Catechol adsorption on TiO_2-B (001) surface, molecular adsorption D0, bi-dentate adsorption D2 and chelating adsorption C1 and C2. Front and side zoomed views.

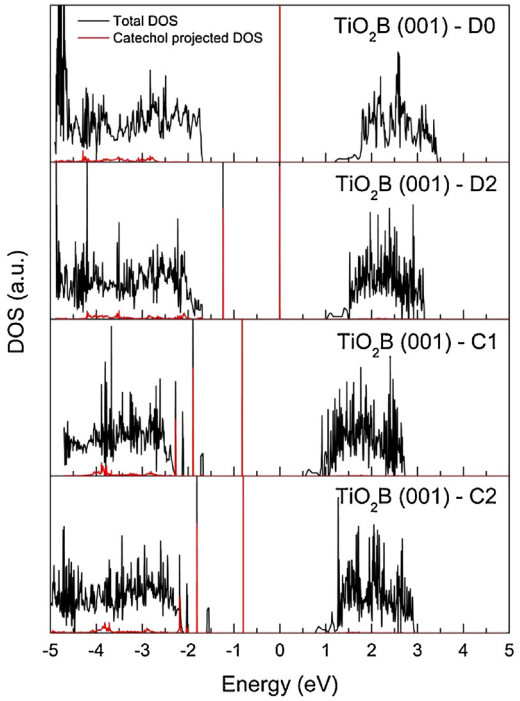

Fig. 6. Total and projected DOS curves for D0, D2, C1 and C2 catechol adsorption on TiO_2-B (001).

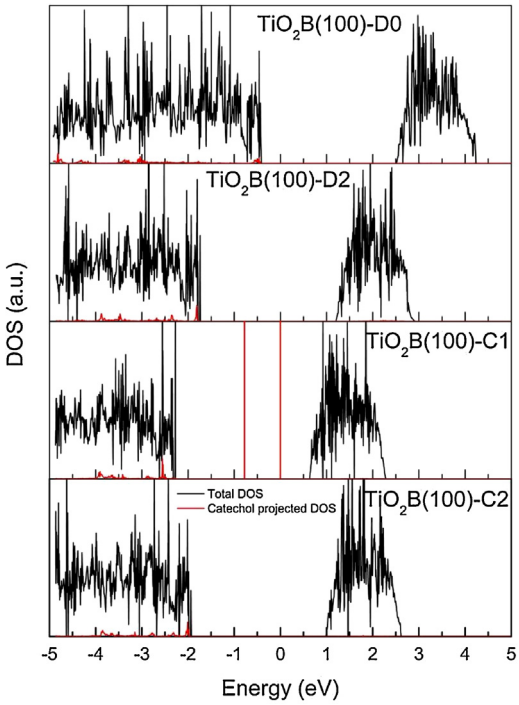

Fig. 8. Total DOS and catechol projected DOS for D0, D2, C1 and C2 adsorption on TiO_2-B (100).

3.2. Frontier orbitals

For an effective sensitization performance, it is very important that the HOMO (highest occupied molecular orbital) of the dye is in the semiconductor gap and the LUMO (lowest unoccupied molecular orbital) is above the conduction band minimum. Thus, the electron-hole separation is achieved in the hybrid interface by electron photo-injection from the dye molecule HOMO to the surface conduction band, or by first excitation of an electron from HOMO to LUMO of the dye follow by electron injection in the surface conduction band. Naturally, catechol on anatase (101) presents this behavior, being classified as DSSC type-II system, in which a direct charge-transfer occurs from dye's HOMO to the semiconductor's CB, that should present a band absorption in the visible region of the electromagnetic spectrum [55,56]. From our studied systems, catechol on hydrogen titanate containing an oxygen vacancy and catechol at C1 location on TiO_2B (100) are the appropriate ones for DSSC applications, due to their favorable adsorption energies and because they fulfill the frontier orbitals condition. In Figs. 9 and 10, as a comparison, front and side view, for HOMO and LUMO, respectively, corresponding to systems dye/anatase (101), dye/hydrogen titanate (100) and dye/TiO_2B(100)-C1 are plotted. It is clear that HOMO is composed from π-states of the dye, and LUMO for Ti-d states of the surface, as expected.

It can be observed in Fig. 9 that HOMO frontier orbital of dye/H-titanate-D1 involves the catechol oxygen atom and one superficial titanium atom, which would make more probable the electron transfer from adsorbate to the semiconductor surface. In D1-vac

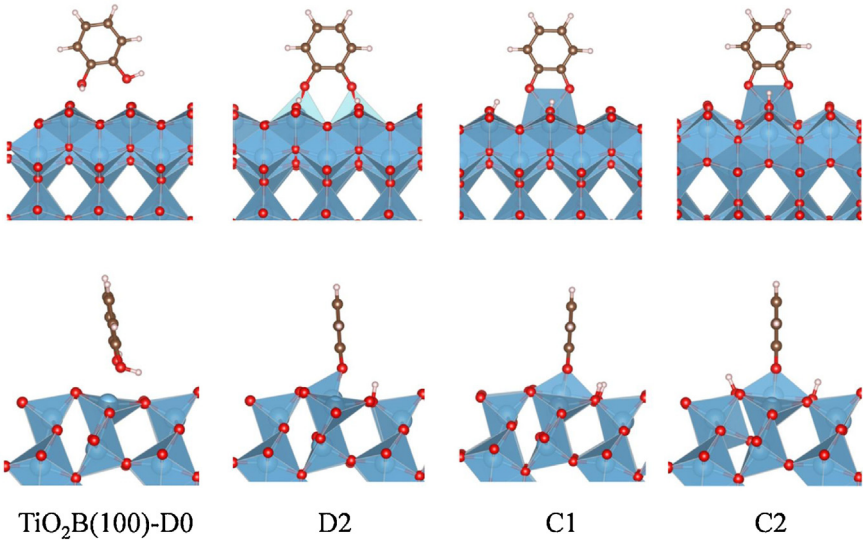

Fig. 7. Catechol adsorption on TiO_2-B (100) surface, molecular adsorption D0, bi-dentate adsorption D2 and chelating adsorption C1 and C2. Front and side zoomed views.

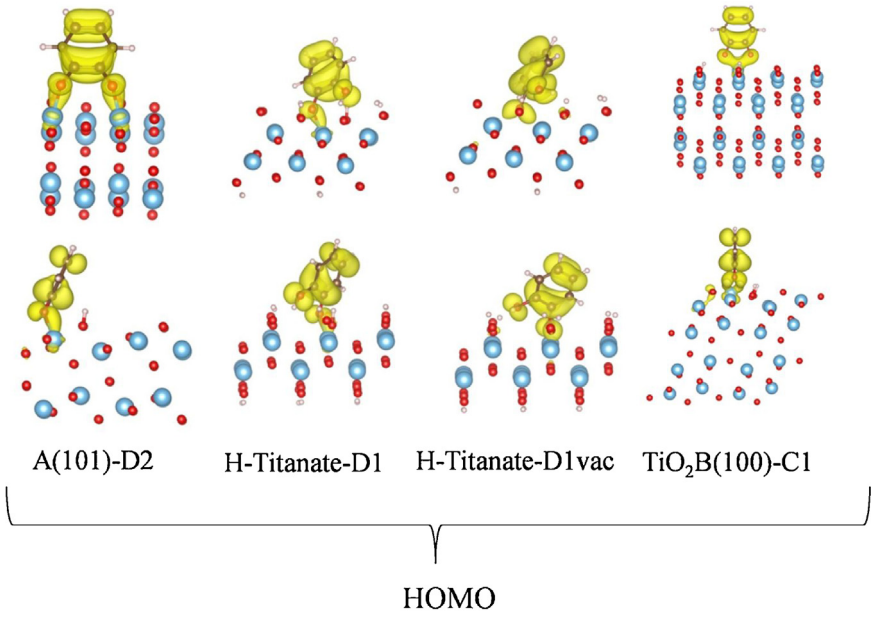

Fig. 9. HOMO frontier orbitals for optimum dye/semiconductor systems. Front and side view are shown. Some bonds were omitted for sake of clarity.

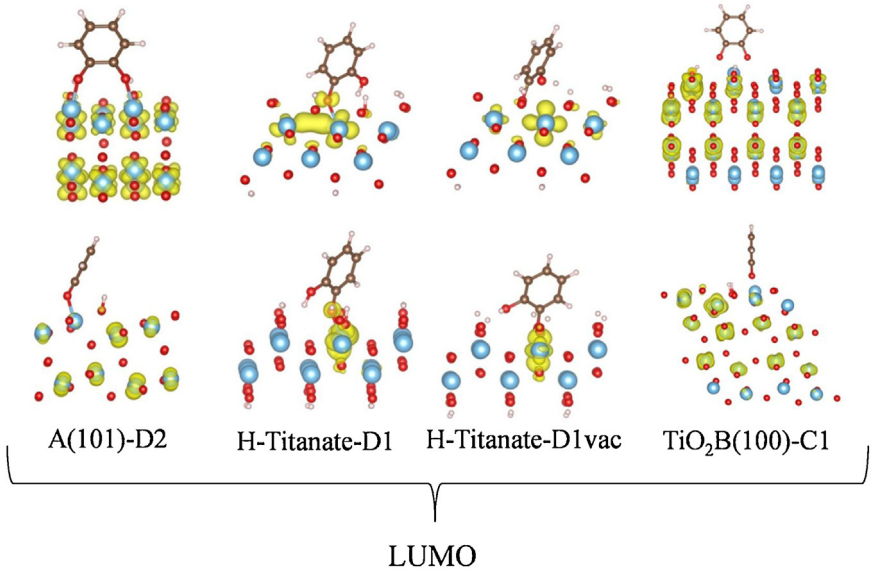

Fig. 10. LUMO frontier orbitals for optimum dye/semiconductor systems. Front and side view are shown. Some bonds were omitted for sake of clarity.

adsorption case, HOMO frontier orbital involves not only the dye oxygen p-states but also titanium d-states from the surface, given that dye oxygen atom occupies now the semiconductor vacancy, turning this surface more stable. However, this oxygen atom coming from the dye can be interpreted now as part of the surface, thus making more difficult the electron transfer process. In the case of dye/TiO_2B(100)-C1 the HOMO orbital overlap is small making the system less appropriate for DSSC applications in comparison with hydrogen titanate surfaces.

Finally, and utilizing the work function information it is possible to perform a first approach to the band alignment of all the reported surfaces as can be observed in Fig. 11. Additionally, taking as a reference the I_2/I_3^- redox pair potential E_{redox}, it is possible to estimate the open circuit potential V_{OC} according to [57]:

$$V_{OC} = \frac{1}{q_e}\left(E_{CB} + k_B T \mathrm{In}\left(\frac{n_c}{N_{CB}}\right) - E_{redox}\right)$$

Where n_c and N_{CB} corresponds to the electrons in the conduction band and the total number of electronic states in the CB, respectively and k_B is the Boltzmann constant. Taking the $\frac{n_c}{N_{CB}}$ ratio as constant for all the surfaces [57], it is possible to draw the scheme presented in Fig. 11. According to this, the V_{OC} ordering is the following: $V_{OC\text{-}TNT(100)} > V_{OC\text{-}TiO2(B)(001)} > V_{OC\text{-}Anatase(101)} > V_{OC\text{-}TiO2(B)(100)}$.

4. Conclusions

The performance of surfaces of new compounds found experimentally –TiO_2-B and $H_2Ti_3O_7$- in DSSC was analyzed by testing their adsorbant properties via dye model catechol adsorption. Structural and electronic properties were calculated using DFT theory, implementing Hubbard U term. It was found that not all these semiconductor surfaces are prone to catechol adsorption and electron transfer from dye to surface. TiO_2-B (001) is not energetically optimum for dye adsorption due to its low (001) surface energy,

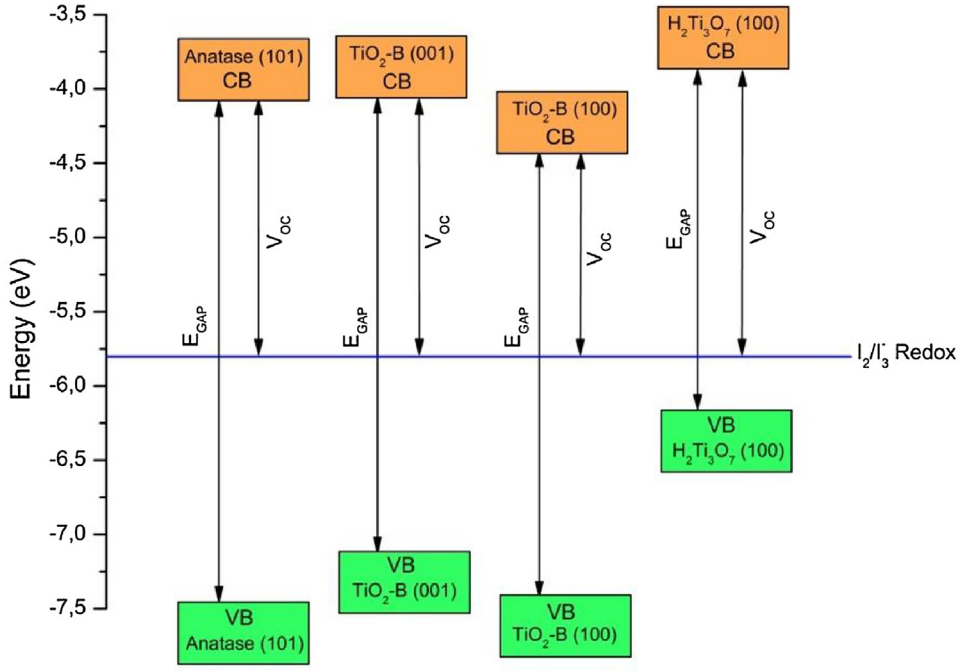

Fig. 11. Band alignment for all the studied polymorphs and titanates, utilizing as reference the I_2/I_3^- redox pair potential.

although the gap from valence band to conduction band is appropriate for electron transfer and well positioned in the visible region of the electromagnetic spectrum. Surface TiO_2-B (100) behaves in the opposite way, showing favorable adsorption energies for D0, D2, C1 and C2 configurations. In particular, TiO_2-B (100)-C1 configuration is energetically possible and involves a considerable small gap for electron transfer. $H_2Ti_3O_7$ (100) surface, containing an oxygen vacancy is the more suitable one for DSSC applications due to its optimum dye adsorption energy and small gap between valence band and conduction band. Frontier orbitals plots endorses this conclusion showing the dye/surface orbitals overlapping in HOMO allowing an easy electron transfer. Finally, the band alignment study allows as to conclude that the H-titanate surfaces should develop the higher open circuit voltage in comparison to the rest of the studied TiO_2 polymorphs.

Acknowledgments

E. G. is a member of CONICET. Authors acknowledge SGCyT (UNS), IFISUR-CONICET, CIC-Buenos Aires, PICT 1770. E. G. would like to thank Agencia Nacional de Investigación e Innovación (ANII) for providing the opportunity to undertake this research by supporting her Post-doc "Fondo Profesor Dr. Roberto Caldeyro Barcia" code PD_NAC_2015_1_108133. A. W. M. and R. F. acknowledge ANII, PEDECIBA and CSIC.

References

[1] R. Marchand, L. Brohan, M. Tournox, TiO_2(B) a new form of titanium dioxide and the potassium octatitanate $K_2Ti_8O_{17}$, Mater. Res. Bull. 15 (1980) 1129–1133.
[2] T.P. Feist, S.J. Mocarski, P.K. Davies, A.J. Jacobson, J.T. Lewandowski, Formation of TiO_2(B) by proton exchange and thermolysis of several alkali metal titanate structures, Solid State Ionics 28–30 (1988) 1338–1343.
[3] T.P. Feist, P.K. Davies, The soft chemical synthesis of TiO_2 (B) from layered titanates, J. Solid State Chem. 101 (1992) 275–295.
[4] L. Qi, Y. Liu, C. Li, Controlled synthesis of TiO_2-B nanowires and nanoparticles for dye-sensitized solar cells, App. Surf. Sci. 257 (2010) 1660–1665.
[5] R. Armstrong, G. Armstrong, J. Canales, R. García, R.G. Bruce, Lithium-Ion intercalation into TiO_2-B nanowires, Adv. Mater. 17 (2005) 862–865.
[6] G. Armstrong, R. Armstrong, P.G. Bruce, P. Reale, B. Scrosati, TiO_2(B) nanowires as an improved anode material for lithium-ion batteries containing $LiFePO_4$ or $LiNi_{0.5}Mn_{1.5}O_4$ cathodes and a polymer electrolyte, Adv. Mater. 18 (2006) 2597–2600.
[7] Q. Wang, Z. Wen, J. Li, A hybrid supercapacitor fabricated with a carbon nanotube cathode and a TiO_2–B nanowire anode, Adv. Funct. Mater. 16 (2006) 2141–2416.
[8] C.C. Tsai, Y.Y. Chu, H. Teng, A simple electrophoretic deposition method to prepare TiO_2–B nanoribbon thin films for dye-sensitized solar cells, Thin Solid Films 519 (2010) 662–665.
[9] J. Qu, X.P. Gao, G.P. Li, Q.W. Jiang, T.Y. Yan, Structure transformation and photoelectrochemical properties of TiO_2 nanomaterials calcined from titanate nanotubes, J. Phys. Chem. C 113 (2009) 3359–3363.
[10] K. Asagoe, S. Ngamsinlapasathian, Y. Suzuki, S. Yoshikawa, Addition of TiO_2 nanowires in different polymorphs for dye-sensitized solar cells, Cent. Eur. J. Chem. 5 (2007) 605–619.
[11] M. Ben Yahia, F. Lemoigno, T. Beuvier, J.S. Filhol, M. Richard-Plouet, L. Brohan, M.L. Doublet, Updated references for the structural, electronic, and vibrational properties of TiO_2(B) bulk using first-principles density functional theory calculations, J. Chem. Phys. 130 (204501) (2009) 1–11.
[12] M. A.Vittadini, M. Casarin, A. Selloni, Structure and stability of TiO_2-B surfaces: a density functional study, J. Phys. Chem. C 113 (2009) 18973–18977.
[13] W. Liu, J.G. Wang, W. Li, X. Guo, L. Lu, X. Lu, X. Feng, C. Liu, Z. Yan, A shortcut for evaluating activities of TiO_2 facets: water dissociative chemisorption on TiO_2-B (100) and (001), Phys. Chem. Chem. Phys. 12 (2010) 8721–8727.
[14] D.V. Bavykin, F.C. Walsh, Titanate and titania nanotubes: synthesis, properties and applications, in: P. O'Brien, H. Kroto, H. Craighead (Eds.), RSC Nanoscience & Technology Series, No. 12, RSC Publishing, Cambridge, U.K, 2010.
[15] A. Vittadini, F. Sedona, S. Agnoli, L. Artiglia, M. Casarin, G.A. Rizzi, M. Sambi, G. Granozzi, Stability of TiO_2 polymorphs: exploring the extreme frontier of the nanoscale, ChemPhysChem 11 (2010) 1550–1557.
[16] M. D'Arienzo, J. Carbajo, A. Bahamonde, M. Crippa, S. Polizzi, R. Scotti, L. Wahba, F. Morazzoni, Photogenerated defects in shape-Controlled TiO_2, J. Am. Chem. Soc. 133 (2011) 17652–17661.
[17] M.J. Elser, O. Diwald, Facilitated lattice oxygen depletion in consolidated TiO_2 nanocrystal ensembles: a quantitative spectroscopic O_2 adsorption study, J. Phys. Chem. C 116 (2012) 2896–2903.
[18] B. Schürer, M.J. Elser, A. Sternig, W. Peukert, O. Diwald, Delamination and dissolution of titanate nanowires: a combined structure and in situ second harmonic generation study, J. Phys. Chem. C 115 (2011) 12381–12387.
[19] H. Zhu, Y. Lan, X.P. Gao, S.P. Ringer, Z.F. Zheng, D.Y. Song, J.C. Zhao, Phase transition between nanostructures of titanate and titanium dioxides via simple wet-chemical reactions, J. Am. Chem. Soc. 127 (2005) 6730–6736.
[20] A. Vittadini, M. Schirmer, M.-M. Walz, F. Vollnhals, T. Lukasczyk, H.-P. Steinrück, H. Marbach, M.J. Elser, B. Schürer, O. Diwald, Defects in oxygen-depleted titanate nanostructures, Langmuir 28 (2012) 7851–7858.
[21] A. Eguía-Barrio, E. Castillo-Martínez, M. Zarrabeitia, M.A. Muñoz-Márquez, M. Casas-Cabanas, T. Rojo, Structure of $H_2Ti_3O_7$ and its evolution during sodium insertion as anode for Na ion batteries, Phys. Chem. Chem. Phys. 17 (2015) 6988–6994.
[22] Y. An, Z. Li, H. Xiang, Y. Huang, J. Shen, First-principle calculations for electronic structure and bonding properties in layered $Na_2Ti_3O_7$, Cent. Eur. J. Phys. 9 (2011) 1488–1492.

[23] D. Szieberth, A.M. Ferrari, P. D'Arco, R. Orlando, Ab initio modeling of trititanate nanotubes, Nanoscale 3 (2011) 1113–1119.
[24] B. O'Regan, M.A. Grätzel, Low-cost, high-efficiency solar cell based on dye sensitized colloidal TiO_2 films, Nature 353 (1991) 737–739.
[25] M. Grätzel, Photoelectrochemical cells, Nature 414 (2001) 338–344.
[26] J.H. Wu, Z. Lan, J.M. Lin, M.L. Huang, S.C. Hao, T. Sato, S.A. Yin, Novel thermosetting gel electrolyte for stable quasi-solid-state dye-sensitized solar cells, Adv. Mater. 19 (2007) 4006–4011.
[27] J. Wu, S. Hao, Z. Lan, J. Lin, M. Huang, Y. Huang, P. Li, S. Yin, T. Sato, An all-Solid-State dye-Sensitized solar cell-Based poly(N-alkyl-4-vinyl-pyridine iodide) electrolyte with efficiency of 5.64%, J. Am. Chem. Soc. 130 (2008) 11568–11569.
[28] L. Dloczik, O. Ileperuma, I. Lauermann, L.M. Peter, E.A. Ponomarev, G. Redmond, N.J. Shaw, I. Uhlendorf, Dynamic response of dye-Sensitized nanocrystalline solar Cells: Characterization by intensity-Modulated photocurrent spectroscopy, J. Phys. Chem. B 101 (1997) 10281–10289.
[29] R. Mosurkal, J.A. He, K. Yang, L.A. Samuelson, J. Kumar, Organic photosensitizers with catechol groups for dye-sensitized photovoltaics, J. Photochem. Photobiol. A 168 (2004) 191–196.
[30] C.R. Rice, M.D. Ward, M.K. Nazeeruddin, M. Grätzel, Catechol as an efficient anchoring group for attachment of Ruthenium–polypyridine photosensitisers to solar cells based on nanocrystalline TiO_2 films, New J. Chem. 24 (2000) 651–652.
[31] P. Persson, R. Bergström, S. Lunell, Quantum chemical study of photoinjection processes in dye-sensitized TiO_2 nanoparticles, J. Phys. Chem. B 104 (2000) 10348–10351.
[32] W.R. Duncan, O.V. Prezhdo, Electronic structure and spectra of catechol and alizarin in the gas phase and attached to titanium, J. Phys. Chem. B 109 (2005) 365–373.
[33] S. Rangan, J.P. Theisen, E. Bersch, R.A. Bartynski, Energy level alignment of catechol molecular orbitals on ZnO(1 1 2 0) and TiO_2(1 1 0) surfaces, Appl. Surf. Sci. 256 (2010) 4829–4833.
[34] R. Sanchez-de Armas, M.A. San-Miguel, J. Oviedo, A. Marquez, J.F. Sanz, Electronic structure and optical spectra of catechol on TiO_2 nanoparticles from real time TD-DFT simulations, Phys. Chem. Chem. Phys. 13 (2011) 1506–1514.
[35] R. Walter, O.V.P. Duncan, Theoretical studies of photoinduced electron transfer in dye-sensitized TiO_2, Annu. Rev. Phys. Chem. 58 (2007) 143–184.
[36] L.G.C. Rego, V.S. Batista, Quantum dynamics simulations of interfacial electron transfer in sensitized TiO_2 semiconductors, J. Am. Chem. Soc. 125 (2003) 7989–7997.
[37] Y. Xu, W.K. Chen, S.H. Liu, M.J. Cao, J.Q. Li, Interaction of photoactive catechol with TiO_2 anatase (1 0 1) surface: a periodic density functional theory study, Chem. Phys. 331 (2007) 275–282.
[38] U. Terranova, D.R. Bowler, Adsorption of catechol on TiO_2 rutile (100): a density functional theory investigation, J. Phys. Chem. C 114 (2010) 6491–6495.
[39] F. Risplendi, G. Cicero, G. Mallia, N.M.A. Harrison, A quantum-mechanical study of the adsorption of prototype dye molecules on Rutile-TiO_2(110): a comparison between catechol and isonicotinic acid, Phys. Chem. Chem. Phys. 15 (2013) 235–243.
[40] D.J. Mowbray, A. Migani, Optical absorption spectra and excitons of dye substrate interfaces: catechol on TiO_2 (110), J. Chem. Theory Comput. 12 (2016) 2843–2852.
[41] L.M. Liu, S.C. Li, H. Cheng, U. Diebold, A. Selloni, A. Growth, Organization of an organic molecular monolayer on TiO_2: catechol on anatase (101), J. Am. Chem. Soc. 133 (2011) 7816–7823.
[42] S.C. Li, Y. Losovyj, U. Diebold, Adsorption-site-dependent electronic structure of catechol on the anatase TiO_2(101) surface, Langmuir 27 (2011) 8600–8604.
[43] S.C. Li, L.N. Chu, X.Q. Gong, U. Diebold, Hydrogen bonding controls the dynamics of catechol adsorbed on a TiO_2(110) surface, Science 328 (2010) 882–884.
[44] S.C. Li, J.G. Wang, P. Jacobson, X.Q. Gong, A. Selloni, U. Diebold, Correlation between bonding geometry and band gap states at organic-inorganic interfaces: catechol on rutile TiO_2(110), J. Am. Chem. Soc. 131 (2009) 980–984.
[45] H.H. Kristoffersen, J.E. Shea, H. Metiu, Catechol and HCl adsorption on TiO_2(110) in vacuum and at the Water–TiO_2 interface, J. Phys. Chem. Lett. 6 (2015) 2277–2281.
[46] D.H. Douma, R. Gebauer, Optical properties of dye sensitized TiO_2 nanowires from time-dependent density functional theory, Phys. Status Solidi RRL 5 (2011) 259–261.
[47] W. Kohn, L.J. Sham, Self-consistent equations including exchange and correlation effects, Phys. Rev. 140 (1965) A1133–A1138.
[48] G. Kresse, J. Furthmuller, Efficiency of ab-initio total energy calculations for metals and semiconductors using a plane-wave basis set, Comput. Mater. Sci. 6 (1996) 15–50.
[49] G. Kresse, D. Joubert, From ultrasoft pseudopotentials to the projector augmented-wave method: phys, Rev. B: Condens. Matter Mater. Phys. 59 (1999) 1758–1775.
[50] P.E. Blöchl, Projector augmented-wave method: phys, Rev. B: Condens. Matter Mater. Phys. 50 (1994) 17953–17979.
[51] B. Hammer, L.B. Hansen, J.K. Nørskov, Improved adsorption energetics within density-functional theory using revised perdew-Burke-Ernzerhof functionals, Phys. Rev. B: Condens. Matter Mater. Phys. 59 (1999) 7413–7421.
[52] S.L. Dudarev, G.A. Botton, S.Y. Savrasov, C.J. Humphreys, A.P. Sutton, Electron-energy-loss spectra and the structural stability of nickel oxide: an LSDA+U study, Phys. Rev. B: Condens. Matter Mater. Phys. 57 (1998) 1505–1509.
[53] E. German, R. Faccio, A.W. Mombrú, A DFT+U study on structural, electronic, vibrational and thermodynamic properties of TiO_2 polymorphs and hydrogen titanate: tuning the Hubbard U-term, J. Phys. Commun. (2017) (sent).
[54] H.J. Monkhorst, J.D. Pack, Special points for brillouin-zone integrations: phys, Rev. B: Condens. Matter Mater. Phys. 13 (1976) 5188–5192.
[55] E.L. Tae, S.H. Lee, J.K. Lee, S.S. Yoo, E.J. Kang, K.B. Yoon, A strategy to increase the efficiency of the dye-Sensitized TiO2 solar cells operated by photoexcitation of dye-to-TiO2 charge-transfer bands, J. Phys. Chem. B 109 (2005) 22513–22522.
[56] R. Sánchez-de-Armas, M.A. San-Miguel, J. Oviedo, J.F. Sanz, Direct vs. indirect mechanisms for electron injection in DSSC: Catechol and alizarin, Comp. Theor. Chem. 975 (2011) 99–105.
[57] S. Bagheri Novir, S.M. Hashemianzadeh, Density functional theory study of new azo dyes with different π-spacers for dye-sensitized solar cells, Spectrochim. Acta, Part A 143 (2015) 20–34.